Experimental Investigation on Edge Inversion at Trivalent Bismuth and Antimony: Great Acceleration by Intra- and Intermolecular Nucleophilic Coordination

Yohsuke Yamamoto, Xiang Chen, Satoshi Kojima, Keisuke Ohdoi, Mutsuko Kitano, Yasutaka Doi, and Kin-ya Akiba*

Contribution from the Department of Chemistry, Faculty of Science, Hiroshima University, 1-3-1 Kagamiyama, Higashi-Hiroshima 724, Japan

Received December 13, 1994[⊗]

Abstract: The activation free energy of inversion at the bismuth atom of the trivalent organobismuth compounds {2-$C_6H_4C(CF_3)_2O$}Bi(4-$CH_3C_6H_4$) (**4a**), {2-$C_6H_4C(CF_3)_2O$}Bi(2-$C_6H_4CH_2NMe_2$) (**10**), and {2-$C_6H_4C(CF_3)_2O$}Bi(2-$C_6H_4CMe_2OMe$) (**11**) in DMSO-d_6 was measured by use of variable temperature ^{19}F NMR and found to be 21.2 (175 °C), 15.4 (55 °C), and 18.6 (125 °C) kcal mol^{-1}, respectively. The corresponding energy of **10** in pyridine decreased to 14.6 (40 °C), whereas that in 2,6-lutidine was 20.6 (170 °C) kcal mol^{-1}. These results imply that intramolecular coordination of the methoxy and the dimethylamino groups and also intermolecular coordination of the pyridine solvent greatly stabilize the transition state of inversion at the bismuth atom. This phenomenon can only be rationalized by the edge inversion mechanism. Inversion at the bismuth atom of {2-$C_6H_4C(CF_3)_2O$}Bi{4-(R)-2,6-$C_6H_2(CH_2NMe_2)_2$} (**21**, R = *t*-Bu; **22**, R = H) bearing two potential intramolecularly coordinating groups was so fast that the barrier could not even be measured at −90 °C. The barrier of the corresponding antimony compound {2-$C_6H_4C(CF_3)_2O$}Sb{2,6-$C_6H_3(CH_2NMe_2)_2$} (**23**) in CD_2Cl_2 was found to be 9.5 kcal mol^{-1} at −70 °C. The M−N dissociation in the NMe_2 group was determined to be 12.3 kcal mol^{-1} for **22** (M = Bi, T_c = −5 °C in toluene-d_8) and 12.0 kcal mol^{-1} for **23** (M = Sb, T_c = −19.2 °C in CD_2Cl_2). Thus, inversion for the bismuth (**22**) and the antimony atom (**23**) can be regarded as taking place without dissociation of the Bi−N (or Sb−N) bonds, that is, via a 12−M−5 (M = Sb and Bi) transition state. X-ray crystallographic analyses of **10**, **22**, and **23** are presented which showed the presence of intramolecular coordination of N and O to the central atom (Bi or Sb).

Introduction

Configurational inversion, in which the ligands around a central group 15 element rearrange without bond cleavage, is common in three-coordinate compounds having a pair of nonbonding electrons. The vertex inversion mechanism which has been generally accepted involves passage through a trigonal transition state, in which configuration at the central atom is sp^2 and the lone pair electrons possess pure p character. It is well-established that the energy barrier of vertex inversion dramatically increases on moving from second-row elements to third- or fourth-row atoms in the periodic table.[1] Therefore, the isolation of three-coordinate P, As, and Sb compounds with three different substituents in a chiral form has been possible.[2] However, for bismuth derivatives neither isolation of chiral compounds nor estimation of inversion energy barriers has been reported, although Bras and Suzuki have reported the configurational stability of several compounds.[3,4]

Recently a new inversion mechanism called edge inversion has been proposed by Dixon and Arduengo.[5] The edge inversion process proceeds by the movement of the edges of a tetrahedron to form a square planar transition state, where a vacant p-type orbital appears (Scheme 1). If one of the substituents of the tetrahedron is a pair of electrons, the structure of transition state is viewed as T-shaped. The edge and vertex inversion barriers for PH_3, PF_3, AsH_3, AsF_3, SbH_3, and SbF_3 have been calculated, and the fluorides have been predicted to prefer edge inversion. It should be noted that the barriers for the edge inversion decrease as one moves down the family, as shown in Table 1.[6,7] For example, the edge inversion barrier for BiF_3 (33.5 kcal mol^{-1}) is lower than that for SbF_3 (37.6 kcal mol^{-1}),[7] for which the vertex inversion barrier (57.9 kcal mol^{-1}) is much higher.[6] The results indicate the possibility that inversion for bismuth(III) compounds with electron-withdrawing groups may take place via the edge inversion process.

The first demonstration of the edge inversion process was carried out by Arduengo et al. by using sterically restricted 8−P−3[8] compound **1**.[9] The activation parameters of the inversion barrier of **1c** could be estimated by magnetization

[⊗] Abstract published in *Advance ACS Abstracts*, March 15, 1995.

(1) (a) Lambert, J. B. *Top. Stereochem.* **1971**, *6*, 19. (b) Rauk, A.; Allen, L. C.; Clementi, E. *J. Chem. Phys.* **1970**, *52*, 4133. (c) Ahlrichs, R.; Keil, F.; Lischka, H.; Kutzelnigg, W.; Staemmler, V. *J. Chem. Phys.* **1970**, *63*, 455. (d) Dixon, D. A.; Marynick, D. S. *J. Am. Chem. Soc.* **1977**, *99*, 6101. (e) Nógrádi, M. *STEREOCHEMISTRY: Basic Concepts and Applications*; Pergamon Press: New York, 1981; p 141.

(2) (a) Pietrusiewicz, K. M.; Zeblocka, M. *Chem. Rev.* **1994**, *94*, 1375. (b) Wild, S. B. In *The Chemistry of Organic Arsenic, Antimony, and Bismuth Compounds*; Patai, S. Ed.; John Wiley: Chichester, 1994; Chapter 3, p 89. (c) Akiba, K.-y.; Yamamoto, Y. In *The Chemistry of Organic Arsenic, Antimony, and Bismuth Compounds*; Patai, S. Ed.; John Wiley: Chichester, 1994; Chapter 20, p 761. (d) Campbell, I. G. M.; White, A. W. *J. Chem. Soc.* **1958**, 1184.

(3) Suzuki, H.; Murafuji, T. *J. Chem. Soc., Chem. Commun.* **1992**, 1143.

(4) (a) Bras, P.; Gen, A. V. D.; Wolters, J. *J. Organomet. Chem.* **1983**, *256*, C1. (b) Bras, P.; Herwijer, H.; Wolters, J. *J. Organomet. Chem.* **1981**, *212*, C7.

(5) (a) Dixon, D. A.; Arduengo, A. J., III; Fukunaga, T. *J. Am. Chem. Soc.* **1986**, *108*, 2461. (b) Dixon, D. A.; Arduengo, A. J., III. *J. Chem. Phys.* **1987**, *91*, 3195.

(6) Dixon, D. A.; Arduengo, A. J., III. *J. Am. Chem. Soc.* **1987**, *109*, 338.

(7) Moc, J.; Morokuma, K. *Inorg. Chem.* **1994**, *33*, 551.

(8) The *N*−*X*−*L* nomenclature system has been previously described: *N* valence shell electrons about a central atom X with *L* ligands. Perkins, C. W.; Martin, J. C.; Arduengo, A. J., III; Lau, W.; Alegria, A.; Kochi, K. *J. Am. Chem. Soc.* **1980**, *102*, 7753.

(9) Arduengo, A. J., III; Dixon, D. A.; Roe, D. C. *J. Am. Chem. Soc.* **1986**, *108*, 6821.

0002-7863/95/1517-3922$09.00/0

Scheme 1

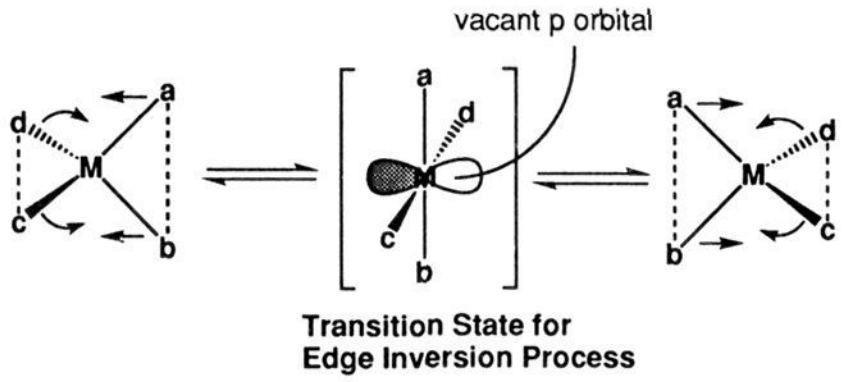

Table 1. Calculated Inversion Barriers (kcal mol^{-1}) for MH_3 and MF_3 (M = P, As, Sb, Bi)

molecule	vertex		edge	
PH_3	35.0[a]	34.7[b]	159.9[a]	
PF_3	85.3[a]		53.8[a]	52.4[b]
AsH_3	41.3[a]	39.7[b]	142.2[a]	
AsF_3	66.3[a]		46.3[a]	45.7[b]
SbH_3	42.8[a]	44.9[b]	112.0[a]	
SbF_3	57.9[a]		38.7[a]	37.6[b]
BiH_3		60.5[b]		
BiF_3				33.5[b]

[a] Reference 6 (MP2). [b] Reference 7 (MP2).

Scheme 2

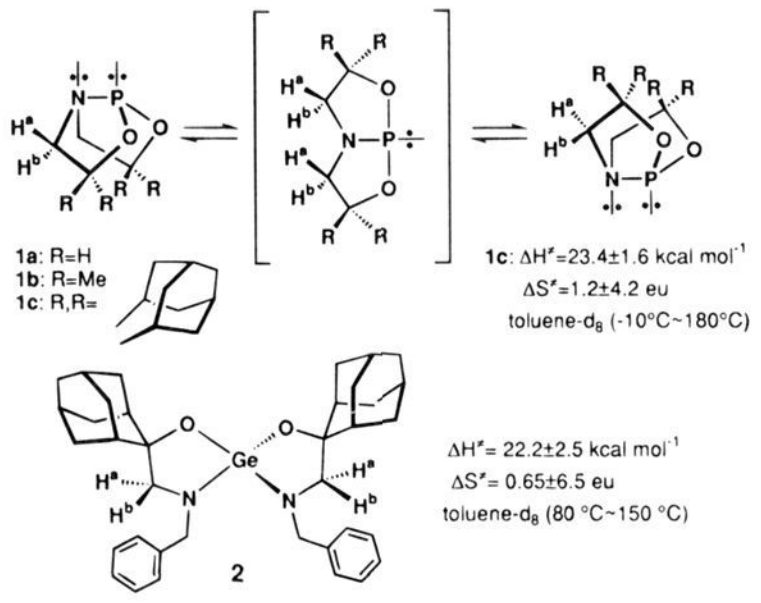

transfer experiments of the H_b multiplet to be $\Delta H^{\ddagger} = 23.4 \pm 1.6$ kcal mol^{-1} and $\Delta S^{\ddagger} = 1.2 \pm 4.2$ eu. The low value for $\Delta S^{\ddagger}$ was consistent with a unimolecular process, as would be expected for simple edge inversion (Scheme 2). Also they were able to determine the barrier of inversion for four-coordinate germanium compound **2**, that is, $\Delta H^{\ddagger}$ was 22.2 kcal mol^{-1} with an activation entropy of 0.65 (±6.51) eu in toluene-d_8.[10]

Another important feature of the edge inversion process is the large reduction of the barrier by nucleophilic association. The vacant p-orbital appearing at the transition state for edge inversion can be stabilized by coordination of external nucleophiles. For example, the edge inversion barrier in phosphoric acid, $PO(OH)_3$, has been calculated to reduce from 69.5 to 38.6 kcal mol^{-1} by coordination of one molecule of NH_3 to the central phosphorus atom in $PO(OH)_3$. The coordination of a second NH_3 could stabilize the transition state by an additional 14.5 kcal mol^{-1} (24.1 kcal mol^{-1} as the barrier).[11]

In this report trivalent organobismuth compounds bearing a hexafluorocumyl alcohol ligand (**3**), the so-called "Martin ligand",[12] are employed for the determination of inversion barriers since an anisochronous pair of the CF_3 groups would be an excellent probe for the configurational exchange at the bismuth center. The barriers and activation parameters, which were mainly determined by NMR line-shape analysis of the CF_3 groups, will be discussed in order to clarify the effect of intramolecularly coordinating nucleophiles and nucleophilic solvents.[13] All data described are consistent with the edge inversion process for the trivalent bismuth(III) and antimony(III) compounds studied.

Scheme 3

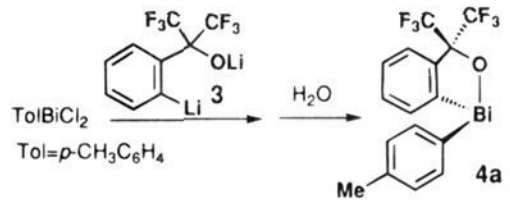

Scheme 4

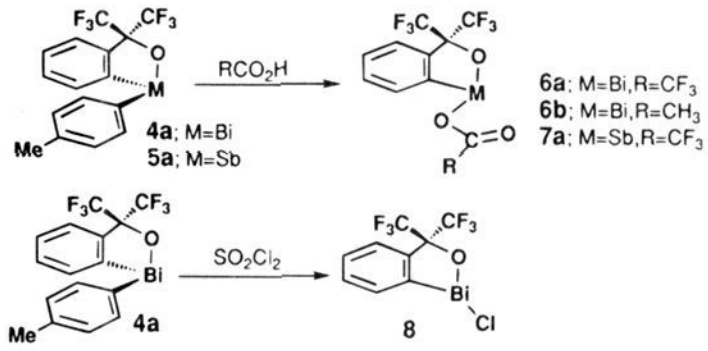

Results and Discusion

Preparation of 1-Substituted 3,3-Bis(trifluoromethyl)-3*H*-2,1-benzoxabismole (4a−4c, 6a, 6b, and 8) and the Antimony Analogues (5a and 7a) and Their Inversion Barriers. 1-(4-Methylphenyl)-3,3-bis(trifluoromethyl)-3*H*-2,1-benzoxabismole (**4a**) was prepared from the dilithio reagent **3** with dichloro(4-methylphenyl)bismuth[14] in 35% yield (Scheme 3). The compound could be purified by column chromatography (SiO_2; *n*-hexane/ethyl acetate = 3/1) and gave correct elemental analysis.

Compounds bearing electronegative acetoxy substituents were prepared by the reaction of **4a** with trifluoroacetic acid or acetic acid. 4-Methylphenyl group was eliminated in preference to the bidentate ligand, and an almost quantitative yield of compound **6a** or **6b** was obtained, respectively (Scheme 4). These compounds were stable to moisture and gave correct elemental analyses. Antimony analogue **5a** also reacted with trifluoroacetic acid to give **7a** quantitatively, however **7a** was found to be susceptible to moisture.

Compounds **6a**, **6b**, or **8** could be used for the reaction with aryllithium to give **4b** and **4c**. Thus, the reaction of **6b** with (4-(trifluoromethyl)phenyl)lithium or (4-methoxyphenyl)lithium at −78 °C gave **4b** or **4c** in the yield of 56% or 34%, respectively (Scheme 5). At higher temperatures, attack at the carbonyl group took place, resulting in the decrease of yields.

The ^{19}F NMR (acetone-d_6) of **4a−c** showed a pair of quartets [e.g., δ −75.7, −78.3 (J = 8.6 Hz) (split width ($\Delta\nu$) 220 Hz) for **4a**] for the CF_3 groups at room temperature, demonstrating that the compound possessed a stable pyramidal configuration. Coalescence of the CF_3 groups of **4a−c** was not observed up to 175 °C in non-nucleophilic solvents such as *o*-dichlorobenzene or benzonitrile. Thus the free energy of activation for the

(10) Arduengo, A. J., III; Dixon, D. A.; Roe, D. C.; Kline, M. *J. Am. Chem. Soc.* **1988**, *110*, 4437.
(11) Dixon, D. A.; Arduengo, A. J., III. *Int. J. Quantum Chem., Symp.* **1988**, *22*, 85.
(12) Perozzi, E. F.; Michalak, R. S.; Figuly, G. D.; Stevenson, W. H., III; Dess, D. B.; Ross, M. R.; Martin, J. C. *J. Org. Chem.* **1981**, *46*, 1049.
(13) Preliminary results have been reported: Yamamoto, Y.; Chen, X.; Akiba, K.-y. *J. Am. Chem. Soc.* **1992**, *114*, 7906.
(14) Gilman, H.; Yablunky, H. L. *J. Am. Chem. Soc.* **1941**, *63*, 207.

Scheme 5

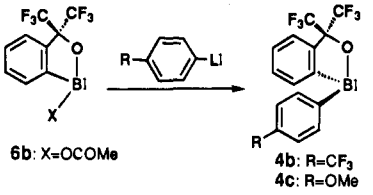

Scheme 6

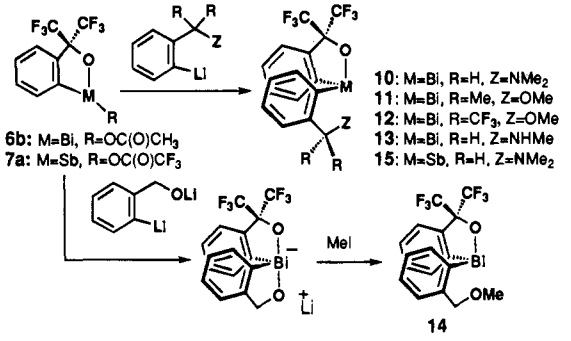

CF_3 exchange could be estimated to be higher than 21−22 kcal mol^{-1} at 175 °C in these solvents.

It was a surprise for us to see a singlet for these CF_3 groups in **6a**, **6b**, and **8** even at −50 °C (acetone-d_6). Hence, the inversion can be regarded as much faster in **6a**, **6b**, and **8** than in **4a**−**c**. These results may suggest that the inversion takes place via the edge inversion process since electronegative substituents should reduce the inversion barrier (vide supra). However, in this case it is also possible that the inversion takes place via an intermolecular process, and in addition an intramolecular process via a four-membered cyclic transition state could also be suggested for **6a** and **6b** by coordination of the carbonyl oxygen to the bismuth atom.

Synthesis of Intramolecularly Coordinated Organobismuth Compounds 10−14 and the Antimony Analogue 15. Preparation of **10**−**13** bearing a Martin ligand and an intramolecularly coordinating substituent was accomplished by the reaction of **6a**, **6b**, or **8** with nucleophiles as shown in Scheme 6. Compound **14** was prepared from *in situ* methylation of 10−Bi−4 ate complex[15] with MeI. Corresponding antimony compound **15** could be prepared from **7a** (Scheme 6).

The fact that ^{19}F NMR spectra of these compounds (**10**−**15**) appeared as one pair of quartets for the CF_3 groups at room temperature shows that the configuration of compounds **10**−**15** is stable. At elevated temperatures we could observe coalescence of this pair of quartets as expected. Before the discussion on the inversion barriers for the compounds, an X-ray crystal structure of **10** is described in the comparison with **11**[15] in order to show the influence of the potential intramolecularly coordinating group on the ground state structure.

Structure of an Intramolecularly Coordinate 10−Bi−4 Compound (10). The X-ray crystal structure determination of **10** shows that the structure of the compound is of pseudotrigonal bipyramid geometry with the NMe_2 group intramolecularly coordinating with the bismuth atom. The lone pair of electrons can be considered to occupy one equatorial position.

The ORTEP drawing of **10** is shown in Figure 1, while selected data on the molecular geometry together with those of **11** are given in Table 2. It is interesting to note here that there is a great similarity in geometry between compounds **10** and **11**. The angles between the apical bonds in **10** and **11** are 160.1-

(15) Chen, X.; Yamamoto, Y.; Akiba, K.-y. *Heteroat. Chem.* **1995**, in press.

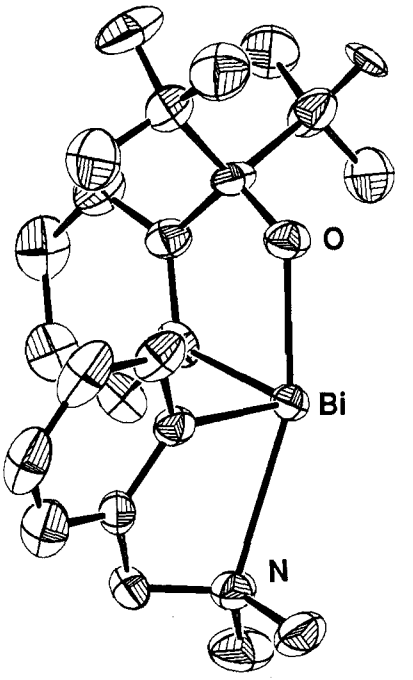

Figure 1. ORTEP diagram (30% probability ellipsoids) for **10**.

Table 2. Selected Distances and Angles for **10** together with **11**

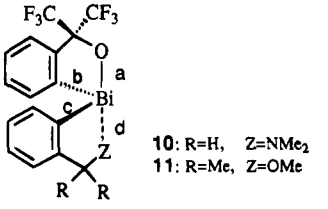

	10	**11**[a]
	Bond Distances (Å)	
a	2.194(9)	2.193(7)
b	2.22(1)	2.24(1)
c	2.236(9)	2.25(1)
d	2.62(1)	2.536(9)
	Bond Angles (deg)	
ab	76.6(4)	76.3(3)
ac	90.2(4)	92.3(3)
ad	160.1(3)	155.2(3)
bc	93.3(4)	94.4(4)
bd	97.5(4)	88.0(3)
cd	71.0(4)	69.5(3)

[a] Reference 15.

(3)° and 155.2(3)°, respectively, and those between the two equatorial carbons are 93.3(4)° and 94.4(4)°, respectively. The apical Bi−O(1) bond distances in **10** (2.194(9) Å) and in **11** (2.193(7) Å) agree very closely with the sum of typical covalent radii of bismuth and oxygen atoms (2.18 Å)[16] but are longer than that of the averaged Bi−O distance found in a three-coordinate monomeric alkoxide complex ($Bi(OC_6H_3Me_2\text{-}2,6)_3$) (2.091 Å).[17] The distance between the bismuth and the nitrogen atom in the NMe_2 group is 2.62(1) Å, which is much shorter than the sum of van der Waals radii (ca. 3.70 Å),[16] demonstrating that the coordination of the NMe_2 group is effective in inducing the formation of a hypervalent 10−Bi−4 compound. The situation is similar for **11**, in which the distance between

(16) Dean, J. A. *Lange's Handbook of Chemistry*, 11th ed.; McGraw-Hill: New York, 1973; pp 3−119. Alcock, N. W. *Adv. Inorg. Radiochem.* **1972**, *15*, 1.

(17) Evans, W. J.; Hain, J. H.; Ziller, J. W. *J. Chem. Soc., Chem. Commun.* **1989**, 1628.

Scheme 7

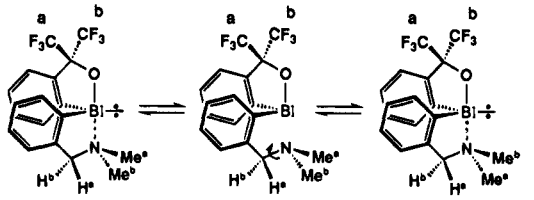

the bismuth and the oxygen atom in the OMe group is 2.536(9) Å, which is much shorter than the sum of the van der Waals radii (ca. 3.67 Å).[16] The distance of the Bi–O(OMe) bond is also longer than that found in four-coordinate 10–Bi–4 compound (**16**) (average 2.30 Å)[18] but is shorter than that of an intermolecularly coordinate compound Ph_2BiBr·THF (2.589(7) Å) recently described.[19] The Bi–N(NMe_2) and Bi–O(OMe) bond lengths in **10** and **11** are elongated by 19% and 16% compared to normal covalent bonds (Bi–N covalent bond length is 2.21 Å[16]), indicating the formation of unsymmetrical hypervalent bonds.[20] In the ^{1}H NMR spectrum of **10**, the methyl protons in the dimethylamino group showed two singlets at 1.74 and 1.85 ppm at low temperatures and coalesced at 37 °C in toluene-d_8 ($\Delta G^{\ddagger}_{37\,°C}$ = 15.4 kcal mol^{-1}). The process observed corresponds to the dissociation–recoordination between the nitrogen and the bismuth atoms that can occur without changing the configuration upon Bi (Scheme 7). The rate-determining step for the coalescence should correspond to the dissociation of Bi–N(NMe_2) bond because the barrier of inversion at a three-coordinate nitrogen atom is known to be small (~6 kcal mol^{-1}).[1]

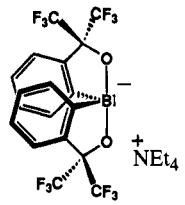

16

Inversion of Configuration at Trivalent Organobismuth Compounds 10–13 Bearing Intramolecularly Coordinate Functional Groups (NMe_2, OMe, NHMe). The inversion of trivalent organobismuth compounds **10–13** could be monitored by ^{19}F NMR for the *gem*-CF_3 groups. After comparison of the experimental spectra with computer-simulated ones,[21] the rate constants obtained were applied to the Eyring equation. In every case the spectra used to obtain the activation parameters were measured at 8 to 13 temperatures so that the statistical errors of $\Delta H^{\ddagger}$ and $\Delta S^{\ddagger}$ were rendered insignificant. In Table 3, coalescence temperatures and the activation parameters in DMSO-d_6 are summarized.

We could also observe the coalescence of methylene protons in the CH_2NMe_2 group of **10** at 2 °C in ^{1}H NMR; the barrier is calculated to be 13.3 kcal mol^{-1} (2 °C) which is consistent with the calculated barrier of 13.5 kcal mol^{-1} at this temperature, on the basis of activation parameters ($\Delta H^{\ddagger}$ and $\Delta S^{\ddagger}$) of **10** calculated from the exchange of the CF_3 groups in ^{19}F NMR. These reduced barriers of inversion in comparison with non-intramolecularly coordinated **4a** ($\Delta G^{\ddagger}_{175\,°C}$ > 21–22 kcal mol^{-1} in *o*-dichlorobenzene and $\Delta G^{\ddagger}_{175\,°C}$ = 21.2 kcal mol^{-1} in DMSO-d_6 (vide infra)) clearly indicate the effect of intramolecularly coordinating groups. It should be noted that the nitrogen nucleophiles stabilized the transition state more than the oxygen nucleophiles (for example, $\Delta G^{\ddagger}_{T_c}$; 15.4 kcal mol^{-1} in **10** vs 18.6 kcal mol^{-1} in **11**). This result can be explained with recourse to donor numbers (DN) since nitrogen nucleophiles have larger DNs than oxygen nucleophiles.[22]

Table 3. Coalescence Temperatures (T_c) and Activation Parameters of Inversion for **10–13** in DMSO-d_6

compd	T_c (°C)	$\Delta G^{\ddagger}_{T_c}$ (kcal mol^{-1})	$\Delta H^{\ddagger}$ (kcal mol^{-1})	$\Delta S^{\ddagger}$ (eu)
10	55	15.4 ± 0.1	11.1 ± 0.6	−12.9 ± 1.8
13	80	16.4 ± 0.1		
11	125	18.6 ± 0.1	12.4 ± 0.3	−15.7 ± 0.7
12	130[a]	19.7 ± 0.1		

[a] Decomposed at 145 °C.

Table 4. Solvent Effect on the Inversion Barrier for **10**

	T_c (°C)	$\Delta G^{\ddagger}_{T_c}$ (kcal mol^{-1})	$\Delta H^{\ddagger}$ (kcal mol^{-1})	$\Delta S^{\ddagger}$ (eu)
toluene-d_8[a]	125	20.5 ± 0.1	12.8 ± 0.4	−18.8 ± 1.0
nitrobenzene[b]	170	20.6 ± 0.1	17.4 ± 0.9	−7.2 ± 2.2
2,6-lutidine[b]	170	20.6 ± 0.1	12.4 ± 0.2	−18.6 ± 0.5
DMSO-d_6[b]	55	15.4 ± 0.1	11.1 ± 0.6	−12.9 ± 1.9
pyridine[b]	40	14.6 ± 0.1	7.1 ± 0.2	−23.6 ± 0.9

[a] Coalescence could be observed only for CH_2 group in ^{1}H NMR. [b] Exchange of the CF_3 groups in ^{19}F NMR was observed.

Scheme 8

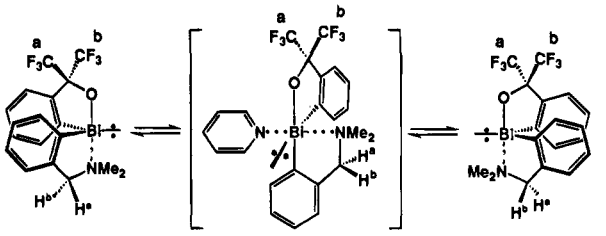

In order to examine whether the inversion barrier is affected by a second external nucleophile, which should reduce the barrier on the basis of the prediction by edge inversion, solvent effects on the barriers of **10** were investigated (Table 4). The dramatic difference between pyridine (T_c = 40 °C, $\Delta G^{\ddagger}_{40\,°C}$ = 14.6 kcal mol^{-1}) and 2,6-lutidine (T_c = 170 °C, $\Delta G^{\ddagger}_{170\,°C}$ = 20.6 kcal mol^{-1}) strongly indicates that the nucleophilic solvent (pyridine) stabilized the transition state in addition to the NMe_2 substituent as shown in Scheme 8. As is evident from Tables 3 and 4, both the intramolecularly coordinating group and nucleophilic solvents reduce the inversion barrier. Thus, these results clearly indicate that two external nucleophiles stabilize the transition state to form a pseudooctahedron, where a pair of configurationally rigid electrons is involved. This cannot be realized with a pentacoordinate transition state formed by coordination of only one nucleophile, which could suffer a series of pseudorotations to effect inversion. The results are consistent with the associated edge inversion transition state.

(18) (a) Chen, X.; Yamamoto, Y.; Akiba, K.-y.; Yoshida, S.; Yasui, M.; Iwasaki, F. *Tetrahedron Lett.* **1992**, *33*, 6653. (b) Yoshida, S.; Yasui, M.; Iwasaki, F.; Yamamoto, Y.; Chen, X.; Akiba, K.-y. *Acta Crystallogr., Sect. B* **1994**, *B50*, 151.

(19) Clegg, W.; Errington, R. J.; Fisher, G. A.; Hockless, D. C.; Normen, N. C.; Orpen, A. G.; Stratford, S. E. *J. Chem. Soc., Dalton Trans.* **1992**, 1967.

(20) Cahill, P. A.; Dykstra, C. E.; Martin, J. C. *J. Am. Chem. Soc.* **1985**, *107*, 6359.

(21) Sandström, J. *Dynamic NMR Spectroscopy;* Academic Press: London, 1982. DNMR 3 program (No. 165QCPE, Kleier, D. A.; Binsch, G.) was used for the simulation: Quantum Chemistry Program Exchange, Indiana Universrsity.

(22) (a) Gutmann, V. *The Donor-Acceptor Approach to Molecular Interactions*; Plenum: New York, 1978. (b) Gutmann, V. *Coord. Chem. Rev.* **1967**, *2*, 239.

Table 5. Substituent and Solvent Effects of Inversion in **4**

compd	solvent	T_c (°C)	$\Delta G^{\ddagger}_{T_c}$ (kcal mol^{-1})	$\Delta H^{\ddagger}$ (kcal mol^{-1})	$\Delta S^{\ddagger}$ (eu)
4a–c	*o*-dichlorobenzene	>175	>21–22		
4a–c	benzonitrile	>175	>21–22		
4a	DMSO-d_6	175	21.2 ± 0.1	11.6 ± 0.4	−21.3 ± 1.0
4a	pyridine-d_5	110	18.0 ± 0.1	9.0 ± 0.1	−23.5 ± 0.4
4b	pyridine-d_5	95	16.8 ± 0.1	8.8 ± 0.1	−21.7 ± 0.3
4c	pyridine-d_5	115	18.2 ± 0.1	11.8 ± 0.2	−16.4 ± 0.5

The barrier of 20.5 kcal mol^{-1} (125 °C) for the inversion of **10** in the nonnucleophilic solvent, toluene-d_8, did not change by dilution of the solution from 0.14 to 0.017 M. The result indicates that the barrier should be that of an intramolecular edge inversion process without solvent participation or intermolecular interaction. It can thus be estimated that the T-shaped transition state is stabilized by at least 5.8 (21.2 (**4a**) − 15.4 (**10**) in DMSO-d_6) kcal mol^{-1} from intramolecular coordination of the NMe_2 group and by 5.9 (20.5 (**10** in toluene-d_8) − 14.6 (**10** in pyridine-d_5)) kcal mol^{-1} from additional coordination by the solvent, i.e., pyridine. It should be noted here that the inversion of **10** in toluene-d_8, which should take place in a five-coordinate form, cannot be rationalized by pseudorotation because the lone pair must be placed at an apical position in one of the inevitable intermediates in the multistep inversion process, and the isolation of chiral 10–S–4 sulfurane (**17**)[23] supports the existence of a high-energy process that inhibits such a permutation.

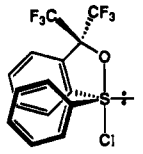

17

Substituent Effect on Edge Inversion at Trivalent Organobismuth Compounds 4a–c in Pyridine-d_5. Since it became evident that nucleophilic solvents reduced the inversion barrier, we tried to observe the inversion of intramolecularly noncoordinate **4a** in nucleophilic solvents. As expected, coalescence could be observed in DMSO-d_6 or pyridine-d_5. Coalescence temperatures and activation parameters are summarized in Table 5.

Also in this case, the barrier for **4a** in pyridine-d_5 ($\Delta G^{\ddagger}_{110\ °C}$ = 18.0 kcal mol^{-1}) is smaller than that in DMSO-d_6 ($\Delta G^{\ddagger}_{175\ °C}$ = 21.2 kcal mol^{-1}) as is expected from DN (29.8 for DMSO, 33.1 for pyridine).[22] Comparison of the rates of **4a** and **4b** in pyridine-d_5 reveals that the rate of inversion is accelerated with increasing σ-electron-withdrawing ability of the substituent (Table 5). This tendency is consistent with the prediction for the edge inversion process that electron-withdrawing groups stabilize the three-center four-electron bond at the T-shaped transition state. The 4-methoxy group, which is a σ-electron-withdrawing and π-donative substituent, is expected to stabilize the three-center four-electron bonding and the vacant p-orbital at the transition state; however the inversion barrier is higher in **4c** (4-$MeOC_6H_4$) than that in **4a** (4-MeC_6H_4). The result indicates that the π-donative substituent, 4-MeO group, may have interfered with the coordination of the solvent, thus leading to an increase in the barrier of inversion. Thus, the effect of solvent coordination may have masked the intrinsic substituent effect in this case. Therefore, we are now trying to measure the barrier of inversion of **18** in nonnucleophilic solvents. As a preliminary result we could determine the barrier of inversion of the diastereomeric **18** at 60 °C in 1,2-dichloroethane to be ca. 27 kcal mol^{-1}.[24]

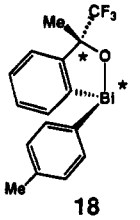

18

Mechanism of Inversion at the Bismuth Center in 10. As was described above, the dissociation of the Bi–N bond in **10** could be measured by the coalescence method and the activation energy was 15.4 kcal mol^{-1} at 37 °C in toluene-d_8. In pyridine-d_5, the signal for the dimethylamino group showed a single peak even at −40 °C (close to the freezing temperature of the solvent); thus, the barrier of dissociation of the Bi–N bond can be estimated to have decreased lower than ca. 11.5 kcal mol^{-1} (at −40 °C). The cause of this decrease might be that the pyridine molecules are able to coordinate with the bismuth atom in the ground state to accelerate the Bi–N dissociation.

The free energies of activation of 20.5 kcal mol^{-1} in toluene-d_8 and 14.6 kcal mol^{-1} in pyridine-d_5 for inversion at the bismuth center are considerably larger than those of the dissociation of the Bi–N bond. Therefore, the rate-limiting step is the inversion and not at all the dissociation of the Bi–N bond.

The inversion process for compound **10** is schematically illustrated in Figure 2. The dissociation of the Bi–N bond takes place before the inversion of the bismuth atom. As the compound moves toward the T-shaped transition state, the NMe_2 group recombines with Bi to stabilize the vacant p-orbital which is perpendicular to the plane. Then the redissociation of the Bi–N bond takes place to give a pyramidal structure with an inverted configuration in which the NMe_2 group interacts with the σ^*_{Bi-O} orbital.

As shown in Tables 4 and 5, the negative and large entropies of activation are consistent with the discussion about the solvent coordination (DMSO-d_6 or pyridine-d_5) and intramolecular coordination of the substituent toward the bismuth atom at the transition state which should increase the absolute value of the negative entropies.

In Figure 2, the value of 14.6 kcal mol^{-1} corresponds to the barrier of the transition state stabilized by the intramolecularly coordinating NMe_2 group and the solvent pyridine. The value of 26–27 kcal mol^{-1} corresponds to the barrier of **18** in 1,2-dichloroethane without any nucleophilic stabilization.

Finally, it is interesting to compare the inversion barrier of bismuth compounds with the corresponding antimony analogues **15**, in which the pair of quartets for the CF_3 groups did not coalesce even in DMSO-d_6 (up to 140 °C) and pyridine-d_5 (up to 80 °C). Thus, the inversion barrier of the antimony analogue **15** is much higher than that of **10** as is expected by the predictions for edge inversion.

(23) Martin, J. C.; Balthazor, T. M. *J. Am. Chem. Soc.* **1977**, *99*, 152.

(24) Kitano, M.; Yamamoto, Y.; Akiba, K.-y. Unpublished results.

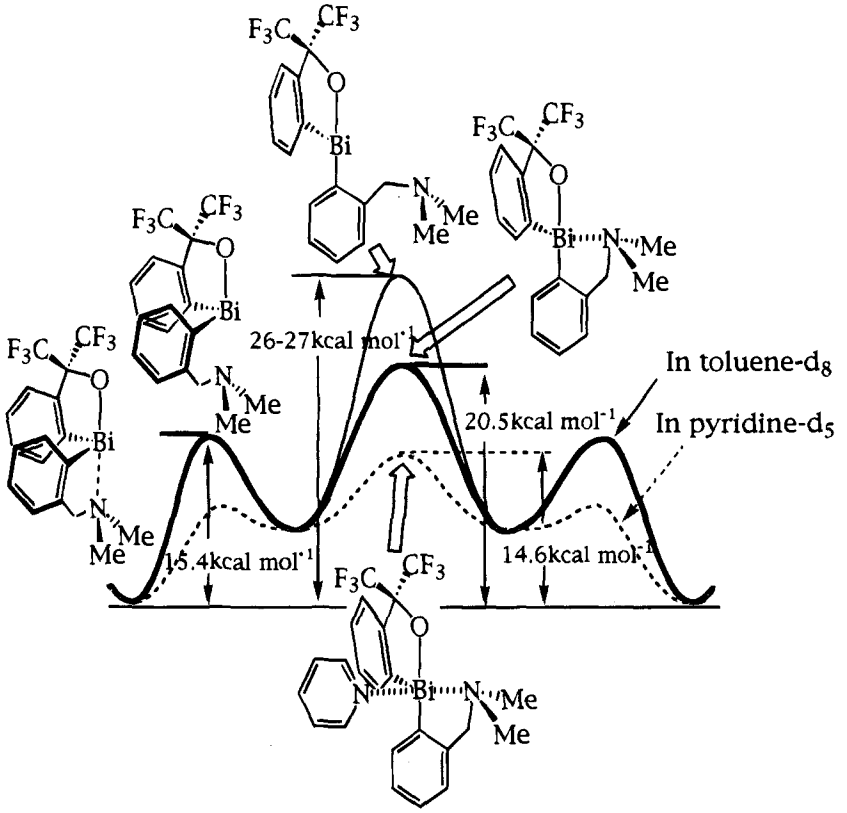

Figure 2. Schematic potential diagram in the inversion of **10**.

Scheme 9

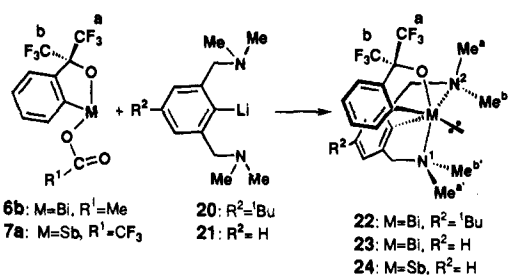

Synthesis and Structure of 12–Bi–5 Bismuth Compounds 22 and 23 with a Tridentate Ligand and the Antimony Analogue 24 and Their Inversion Barriers. In the previous section, we could conclude that the participation of two groups of nucleophiles could reduce the inversion barrier. Therefore, in compounds bearing two potential intramolecularly coordinating groups,[25] very fast inversion was expected to take place. In fact, as an extreme case Arduengo et al. reported compound **19**, which was so stabilized by internally nucleophilic solvation that an edge inversion "transition state" had become a ground state.[26] In order to confirm this hypothesis, compound **22** was synthesized from the reaction of **6b** with **20** as shown in Scheme 9.

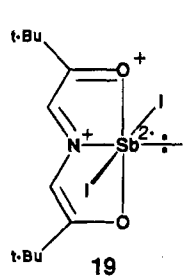

19

The ^{1}H NMR (CD_2Cl_2) spectra of **22** showed a very symmetrical pattern even at −90 °C, one AB pattern for the benzylic protons and two sharp singlets for methyl protons in the NMe_2 group in the ^{1}H NMR spectrum, and notably only one singlet for the CF_3 groups was observed in the ^{19}F NMR spectrum. Therefore, the inversion can be considered to be taking place very rapidly even at −90 °C. At elevated temperatures, the two singlets for the methyl protons in the NMe_2 group coalesced at −17.5 °C. The barrier for the dissociation of either one of the Bi–N bonds is calculated to be 11.8 kcal mol^{-1} at the temperature. Thus, in **22** the barrier of inversion is much lower than that of Bi–N dissociation (Scheme 10).

Scheme 10

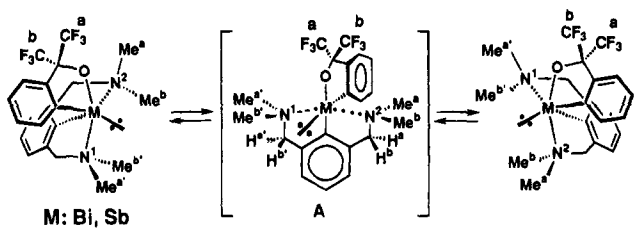

In order to get information about the ground state structure for **22**, we tried to obtain crystals for structural analysis. But **22** did not give any suitable crystals, even after several trials by changing the crystallization conditions such as solvents and temperatures. Therefore, we synthesized **23** instead of **22** with the hope of getting suitable crystals of **23**. The spectral behavior of **23** was essentially the same as that of **22**. To our great

(25) (a) van Koten, G. *Pure Appl. Chem.* **1990**, *62*, 1155. (b) van Koten, G. *Pure Appl. Chem.* **1989**, *61*, 1681. (c) van Koten, G.; Terheijden, J.; van Beek, J. A. M.; Wehman-Ooyevaar, I. C. M.; Muller, F.; Stan, C. H. *Organometallics* **1990**, *9*, 903. (d) van Koten, G.; Jastrzebski, J. T. B. H.; Noltes, J. G.; Spek, A. L.; Shoone, J. C. *J. Organomet. Chem.* **1978**, *148*, 233. (e) Yoshifuji, M.; Otoguro, A.; Toyota, K. *Bull. Chem. Soc. Jpn.* **1994**, *67*, 1503.

(26) Arduengo, A. J., III; Lattman, M.; Dias, H. V. R.; Calabrese, J. C.; Kline, M. *J. Am. Chem. Soc.* **1991**, *113*, 1799.

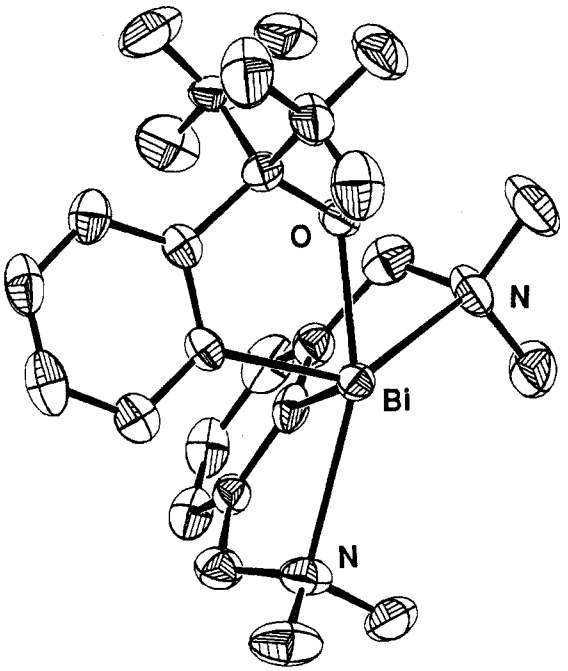

Figure 3. ORTEP diagram (30% probability ellipsoids) for **23**.

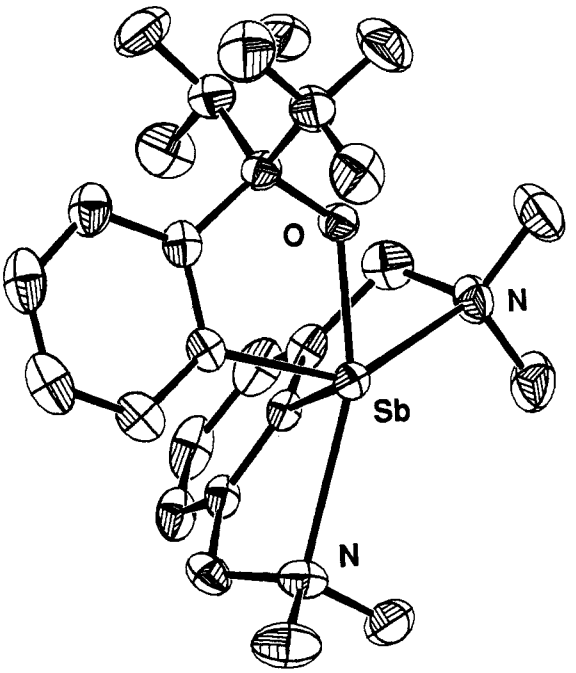

Figure 4. ORTEP diagram (30% probability ellipsoids) for **24**.

Table 6. Selected Distances and Angles for **23** and **24**

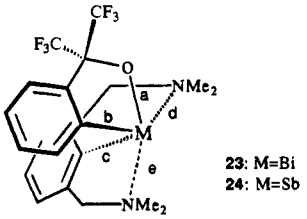

	23	24
	Bond Distances (Å)	
a	2.192(7)	2.067(2)
b	2.30(1)	2.200(1)
c	2.27(1)	2.167(3)
d	2.86(1)	2.844(3)
e	2.68(1)	2.655(2)
	Bond Angles (deg)	
ab	75.2(4)	77.77(4)
ac	94.4(4)	94.46(4)
ad	66.5(3)	67.41(8)
ae	158.1(4)	159.92(9)
bc	96.2(4)	96.6(1)
bd	136.0(4)	139.87(9)
be	90.8(4)	90.3(1)
cd	67.0(4)	67.9(1)
ce	70.0(4)	70.66(9)
de	117.6(3)	116.24(8)

delight, single crystals of **23** were obtained by crystallization from MeOH or CH_3CN.

The X-ray diffraction study of **23** clearly showed an unsymmetrical structure with five-coordination including two nitrogen–bismuth interactions (Figure 3). The selected bond distances and angles are listed in Table 6. The distances between the nitrogen atoms of the *N,N*-dimethylamino groups and the central bismuth are 2.68(1) and 2.86(1) Å, both of which are much shorter than the sum of van der Waals radii (ca. 3.70 Å).[16] The bismuth center can be described as a very distorted octahedron with an electron pair presumably occupying a site trans to the Bi–C bond in the tridentate ligand. It has been reported that in transition metal complexes containing the tridentate ligand, the two nitrogen atoms usually occupy trans positions (180°) and are forced to lie more or less coplanar to the aryl moiety.[25] However, in compound **23** distortion of the N–Bi–N angle (117.6°) and distortion of the nitrogens from the aryl plane are evident. The Bi–O bond distance is equal to that of compound **10** (see Table 2) while other Bi–N (or Bi–C) bond distances in **23** are longer than those of **10** by 2.2–2.8%. The angles of O–Bi–C_{Ar} and C–Bi–C are greater by 4.2° and 2.9° than those of **10**, respectively.

As described above, the ^{19}F NMR spectrum of **23** showed a singlet for the CF_3 groups even at −90 °C; thus the inversion barrier at the bismuth atom can be calculated to be lower than 8 kcal mol^{-1} on the basis of the width of peak separation ($\Delta\nu$ = 692 Hz) in the corresponding antimony compound **24** (vide infra). However, we could observe coalescence for the Me_a and Me_b protons of the NMe_2 group in **23** at −5 °C in toluene-d_8 and at −14 °C in pyridine-d_5. The activation energies for the dissociation of either one of the Bi–N bonds at these temperatures were 12.3 kcal mol^{-1} ($\Delta\nu$ = 245 Hz in toluene-d_8) and 11.9 kcal mol^{-1} ($\Delta\nu$ = 245 Hz in pyridine-d_5), respectively. Thus, the barrier of inversion must be much lower than that of dissociation of either Bi–N bond. We were able to observe still another coalesence for the methylene protons (H_a and H_b) of **23** in toluene-d_8 at 100 °C, and the activation energy at this temperature is calculated to be 16.6 kcal mol^{-1} ($\Delta\nu$ = 681 Hz). This observation can only be rationalized by the dissociation of *both* Bi–N bonds followed by the rotation of the Bi–C (ligand) bond.

The antimony analogue **24** could be prepared similarly and showed similar ^1H and ^{19}F NMR spectra to that of **23** at room temperature in CD_2Cl_2.[27]

The X-ray diffraction study of **24** showed essentially the same structure as **23** (almost overlapped with **23**), that is, a pseudooctahedron bearing two nitrogens coordinating to the antimony atom with the lone pair electrons trans to the Sb–C bond in the tridentate ligand (Figure 4 and Table 6). The distances between the nitrogen of the *N,N*-dimethylamino groups and the central antimony were 2.655(2) and 2.844(3) Å, both of which were much shorter than the sum of the van der Waals radii (ca. 3.6 Å).

(27) Reaction of **20** with $SbCl_3$ has been reported: Atwood, D. A.; Cowley, A. H.; Ruiz, J. *Inorg. Chim. Acta* **1992**, *198–200*, 271.

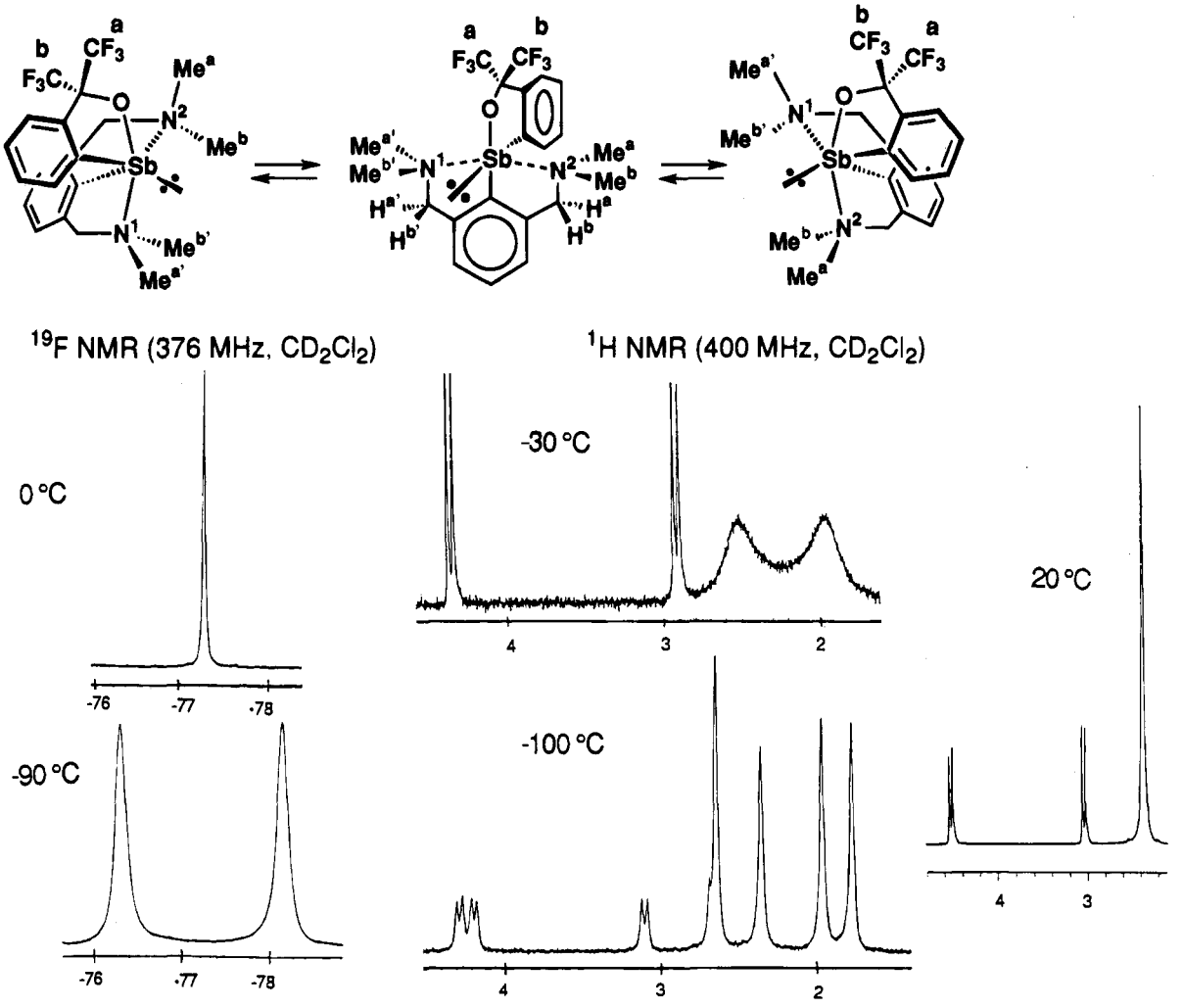

Figure 5. Variable temperature ^1H NMR and ^{19}F NMR spectra of **24**.

Table 7. Coalescence Temperatures (T_c) and Activation Parameters of Inversion for **24** in CD_2Cl_2

	CH_2		Me		CF_3	
δ (rt)	4.42 (H_b, $H_{b'}$) 2.94 (H_a, $H_{a'}$) $J = -14$ Hz		δ (rt)	2.38 (s)	δ (rt)	−75.8 (s)
			δ (227 K)	2.55 (s), 1.92 (s)	δ (196 K)	−74.1 (q) −77.4 (q)
δ (181 K)	4.29 ($H_{b'}$), 4.19 (H_b) 3.11 (H_a), 2.66 ($H_{a'}$) $J_{HaHb} = -15$ Hz $J_{Ha'Hb'} = -14$ Hz		δ (181 K)	2.65 (s), 2.36 (s) 1.97 (s), 1.79 (s)		$J_{FF} = 8$ Hz
T_c (K)	190.3 ($H_bH_{b'}$)	205.4 ($H_aH_{a'}$)	203.9 ($Me_aMe_{a'}$)	199.4 ($Me_bMe_{b'}$)	217.6	
$\delta\nu$ (Hz)	40.0	180.0	111.3	70.3	692.0	
$\Delta G^{\ddagger}_{T_c}$ (kcal mol^{-1})	9.3	9.4	9.5	9.5	9.4	
$\Delta G^{\ddagger}_{203}$(kcal mol^{-1})	9.4		9.5		9.5	
$\Delta H^{\ddagger}$ (kcal mol^{-1})	9.4		9.3		9.3	
$\Delta S^{\ddagger}$(eu)	0.0		−0.5		−1.7	

For **24**, however, we were able to determine the inversion barrier at low temperatures in CD_2Cl_2. Thus, the ^{19}F NMR spectrum showed one pair of quartets for the CF_3 groups, *two* AB patterns were observed for benzylic protons, and four methyl signals were observed for the NMe_2 group at −100 °C, as shown in Figure 5. The observations below −90 °C are consistent with those of the structure in the solid phase. The coalescence temperatures and activation parameters are summarized in Table 7. The fact that all the three coalescences for the three different groups had the same activation energy of 9.5 kcal mol^{-1} at −70 °C can certainly be ascribed to one concerted process, that is, inversion. The small entropies of activation (from 0 to −1.7 eu) are consistent with a process without dissociation of the Sb−N bonds.

It should be noted that the barrier for dissociation for either one of the Sb−N bonds in the NMe_2 group was determined to be 12.0 kcal mol^{-1} (T_c = −19.2 °C) in CD_2Cl_2, which was also much higher than that for inversion at the antimony atom. Thus, inversion for the bismuth (**23**) and the antimony atom (**24**) can be regarded as taking place without dissociation of the Bi−N (or Sb−N) bonds, that is, via a 12−M−5 (M = Sb and Bi) transition state, where a vacant p-type orbital is coordinated by two pairs of lone pair electrons of the nitrogens to generate a three-center four-electron bond.

Table 8. Coalescence Temperatures (T_c) and Activation Free Energies of Inversion for **24** in Toluene-d_8

	CH_2		Me		CF_3
T_c (K)	219 ($H_bH_{b'}$)	230 ($H_aH_{a'}$)	230 ($Me_aMe_{a'}$)	215 ($Me_bMe_{b'}$)	237
$\Delta\nu$ (Hz)	180	412	332	86	620
$\Delta G^{\ddagger}_{T_c}$ (kcal mol^{-1})	10.1	10.2	10.3	10.2	10.4

A measurement with toluene-d_8 as solvent gave similar activation energy values (ca. 10.2 kcal mol^{-1} at −43 °C) as shown in Table 8. The barrier for the Sb−N dissociation in the NMe_2 group was determined to be 12.1 kcal mol^{-1} (T_c = −7 °C) in toluene-d_8. We were able to observe another coalesence for the methylene protons (H_a and H_b) of **24** in toluene-d_8 at 106 °C, which corresponds to the dissociation of *both* Sb−N bonds followed by the rotation of the Sb−C (ligand) bond. The activation energy at this temperature is calculated to be 16.8 kcal mol^{-1} ($\Delta\nu$ = 732 Hz), which is essentially the same as that for **23** (16.6 kcal mol^{-1} at 100 °C) as described above.

A pyridine−CD_2Cl_2 (1:9) solution did not lower the activation energy, thus implying that in this case external nucleophiles have little effect on the inversion process of **23** and **24**.

Experimental Section

Melting points were taken on a Yanagimoto micro melting point apparatus and are uncorrected. ^{1}H NMR (400-MHz), ^{19}F NMR (376-MHz), and ^{13}C NMR (100-MHz) spectra were recorded on a JEOL EX·400 spectrometer. ^{1}H NMR (90-MHz) and ^{19}F NMR (85-MHz) spectra were recorded on a Hitachi R·90H spectrometer. Chemical shifts are reported (δ scale) from internal tetramethylsilane for ^{1}H and ^{13}C or from fluorotrichloromethane for ^{19}F. IR spectra were recorded on a Shimadzu 460 spectrometer. Elemental analysis was performed on a Perkin-Elmer 2400CHN elemental analyzer. Flash column chromatography was carried out on Merck silica gel 9385. Thin·layer chromatography was performed with Merck silica gel GF-254 plates. All reactions were carried out under N_2 or Ar. The preparation of the dilithio derivative of bis(trifluoromethyl)benzyl alcohol[12] followed published procedures. Tetrahydrofuran (THF) and diethyl ether were distilled from sodium/benzophenone.

1-(4-Methylphenyl)-3,3-bis(trifluoromethyl)-3*H*-2,1-benzoxabismole (4a). The dilithio reagent **3**,[12] which was prepared from bis(trifluoromethyl)benzyl alcohol (7 mL, 41.9 mmol), *n*-BuLi (84.2 mmol in 51 mL of hexane), *N,N,N',N'*-tetramethylethylenediamine (TMEDA, 1 mL, 6.4 mmol), and a small amount (ca. 2 mL) of THF, was dissolved in 20 mL of ether and was added dropwise to a cold (−78 °C) stirred suspension of 4-$CH_3C_6H_4BiCl_2$ (TolBiCl$_2$), which was prepared *in situ* by the reaction of Tol_3Bi (6.84 g, 14.2 mmol) with $BiCl_3$ (8.94 g, 28.4 mmol) in ether (120 mL).[14] The mixture was allowed to warm to room temperature and was stirred for a further 12 h. After the reaction was quenched with water, compound **4a** was subjected to column chromatography (*n*·hexane/ethyl acetate = 3/1) to afford colorless crystals (7.95 g, yield 35%). **4a**: mp > 300 °C; ^{1}H NMR (acetone-d_6) 2.24 (s, 3 H), 7.29−8.14 (m, 8 H); ^{19}F NMR (acetone·d_6) −75.7 (q, J = 8.6 Hz, 3 F), −78.3 (q, J = 8.6 Hz, 3 F). Anal. Calcd for $C_{16}H_{11}F_6OBi$: C, 35.44; H, 2.04. Found: C, 35.39; H, 1.98.

1-(4-Methylphenyl)-3,3-bis(trifluoromethyl)-3*H*-2,1-benzoxastibole (5a). The dilithio reagent **3**, which was prepared from bis(trifluoromethyl)benzyl alcohol (6.68 mL, 40.0 mmol), *n*-BuLi (83 mmol in 52 mL of hexane), *N,N,N',N'*-tetramethylethylenediamine (TMEDA, 1.21 mL, 7.81 mmol), and a small amount (ca 2 mL) of THF, was dissolved in 100 mL of THF and was added dropwise to a cold (−78 °C) stirred solution of $TolSbCl_2$ (11.28 g, 40.0 mmol) in THF (100 mL). The mixture was allowed to warm to room temperature and was stirred for a further 12 h. After the reaction was quenched with water, compound **5a** was subjected to column chromatography (*n*-hexane/ethyl acetate = 10/1) to afford colorless crystals (14.19 g, yield 78%). **5a**: mp 113.5−115 °C; ^{1}H NMR ($CDCl_3$) 7.05−7.54 (m, 4 H), 2.25 (s, 3 H); ^{19}F NMR ($CDCl_3$) −75.1 (q, J = 9.3 Hz, 3 F) −77.3 (q, J = 9.3 Hz, 3 F). Anal. Calcd for $C_{16}H_{11}F_6OSb$: C, 42.24; H, 2.44. Found: C, 42.39; H, 2.51.

1-(Trifluoroacetoxy)-3,3-bis(trifluoromethyl)-3*H*-2,1-benzoxabismole (6a). Trifluoroacetic acid (0.02 mL, 0.26 mmol) was added to a solution of **4a** (50.2 mg, 0.093 mmol) in 10 mL of ether at room temperature, and the reaction mixture was stirred for 1 h. Colorless crystals of **6a** were obtained (47 mg, yield 90%) after recrystallization from acetone−ether: mp 185−186 °C; ^{1}H NMR (acetone-d_6) 7.62−7.78 (m, 1 H), 8.04−8.41 (m, 2 H), 8.64−8.78 (m, 1 H); ^{19}F NMR (acetone-d_6) −74.0 (s, 3 F), −74.5 (s, 6 F). Anal. Calcd for $C_{11}H_4F_9O_3$·Bi: C, 23.96; H, 0.89. Found: C, 23.67; H, 0.78.

1-Acetoxy-3,3-bis(trifluoromethyl)-3*H*-2,1-benzoxabismole (6b). Acetic acid (1.0 mL, 22.8 mmol) was added to a solution of **4a** (42.6 mg, 0.079 mmol) in 10 mL of ether at room temperature, and the reaction mixture was stirred for 1 h. Colorless crystals of **6b** were obtained (38 mg, yield 95%) after recrystallization from acetone−ether. The crystalline **6b** with one molecule of acetic acid as crystal solvent was confirmed by elemental analysis and X-ray crystallography.[28] Anal. Calcd for $C_{11}H_7F_6O_3Bi + C_2H_4O_2$: C, 27.38; H, 1.94. Found: C, 27.75; H, 1.98.

The same sample was further dried under vacuum with heat (ca. 100 °C) for 3 h. A colorless powder of **6b** without acetic acid was obtained. **6b**: mp 267−269 °C dec; ^{1}H NMR (acetone-d_6) 1.86 (s, 3 H), 7.53−7.72 (m, 1 H), 7.93−8.25 (m, 2 H), 8.52−8.63 (m, 1 H); ^{19}F NMR (acetone-d_6) −74.8 (s, 6 F). Anal. Calcd for $C_{11}H_7F_6O_3Bi$: C, 25.90; H, 1.38. Found: C, 26.04; H, 1.37.

1-Chloro-3,3-bis(trifluoromethyl)-3*H*-2,1-benzoxabismole (8). Sulfuryl chloride (1.0 mL, 12.4 mmol) was added to a cold (−78 °C) stirred suspension of **4a** (190 mg, 0.35 mmol) in 5 mL of CH_2Cl_2. The mixture was allowed to warm to room temperature and was stirred for a further 3 h. Colorless solid **8** (169 mg, yield 99%) was obtained after evaporation of the solvent *in vacuo*: mp 130 °C dec; ^{1}H NMR (acetone-d_6) 7.60−7.77 (m, 1 H), 8.00−8.33 (m, 2 H), 9.14−9.24 (m, 1 H); ^{19}F NMR (acetone-d_6) −74.3 (s, 6 F).

1-(4-(Trifluoromethyl)phenyl)-3,3-bis(trifluoromethyl)-3*H*-2,1-benzoxabismole (4b). To a stirred solution of **6b** (1.02 g, 2.00 mmol) in ether (30 mL) at −78 °C was added 1.2 equiv of (4-(trifluoromethyl)·phenyl)lithium, which was prepared from 4·(trifluoromethyl)phenyl bromide (0.5 mL, 3.57 mmol) and *n*-BuLi (3.63 mmol in 2.2 mL of *n*-hexane) in ether (10 mL). The mixture was stirred for 3 h at −78 °C, the reaction was quenched with water, and the products were extracted with ether. Colorless crystals of **4b** were obtained after recrystallization from ether−*n*-hexane (0.678 g, yield 56%): mp 223−225 °C (ether−*n*-hexane); ^{1}H NMR (acetone-d_6) 6.95−8.40 (m, 8 H); ^{19}F NMR (acetone-d_6) −63.6 (s, 3 F), −75.1 (q, J = 8.6 Hz, 3 F), −77.6 (q, J = 8.6 Hz, 3 F). Anal. Calcd for $C_{16}H_8F_9OBi$: C, 32.23; H, 1.35. Found: C, 32.25; H, 1.29.

1-(4-Methoxyphenyl)-3,3-bis(trifluoromethyl)-3*H*-2,1-benzoxabismole (4c). To a stirred solution of **6b** (2.13 g, 4.17 mmol) in ether (30 mL) was added at −78 °C 1.2 equiv of (4-methoxyphenyl)lithium, which was prepared from 4-methoxyphenyl bromide (0.7 mL, 5.59 mmol) and *n*-BuLi (4.95 mmol in 3.0 mL of *n*·hexane) in ether (10 mL). The mixture was stirred for 3 h at −78 °C, the reaction was quenched with water, and the products were extracted with ether. Colorless crystals of **4c** (0.79 g, yield 34%) were obtained after recrystallization from acetone·ether. **4c**: mp > 300 °C; ^{1}H NMR (acetone·d_6) 3.76 (s, 3 H), 7.05 (d, J = 7.8 Hz, 2 H), 7.58−7.61 (m, 1 H), 7.81−7.83 (m, 1 H), 7.91−7.93 (m, 1 H), 8.05−8.11 (m, 3 H); ^{19}F NMR (acetone-d_6) −74.3 (q, J = 8.4 Hz, 6 F), −76.8 (q, J = 8.4 Hz, 6 F). Anal. Calcd for $C_{16}H_{11}O_2F_6Bi$: C, 34.42; H, 1.98. Found: C, 34.13; H, 1.91.

1-[2-((*N,N*-Dimethylamino)methyl)phenyl]-3,3-bis(trifluoromethyl)-3*H*-2,1-benzoxabismole (10). To a stirred solution of *N,N*-dimethylbenzylamine (0.8 mL, 6 mmol) in 10 mL of ether at −78 °C was added dropwise *n*·BuLi (6.6 mmol in 4 mL of hexane). The mixture was allowed to warm to room temperature and was stirred for a further 10 h. A solution of **6b** (2.20 g, 4.5 mmol) in 20 mL of ether was added dropwise to a cold stirred solution of the lithium reagent at −78 °C, the mixture was stirred for 6 h, and the reaction was quenched with water. Colorless crystals of **10** (1.58 g, yield 60%) were obtained after

(28) Chen, X.; Yamamoto, Y.; Akiba, K.-y. Unpublished results.

recrystallization from ether: mp 194−195 °C; ^{1}H NMR (acetone-d_6) 2.75 (s, 6 H), 4.04 (d, J = 15 Hz, 1 H), 4.09 (d, J = 15 Hz, 1 H), 7.23−7.29 (m, 6 H), 8.00−8.25 (m, 2 H); ^{19}F NMR (acetone-d_6) −73.1 (q, J = 8.3 Hz, 3 F), −76.5 (q, J = 8.3 Hz, 3 F). Anal. Calcd for $C_{18}H_{16}F_6NOBi$: C, 36.94; H, 2.76; N, 2.39. Found: C, 37.22; H, 2.45; N, 2.24.

1-[2-(2-Methoxy-2-propyl)phenyl]-3,3-bis(trifluoromethyl)-3*H*-2,1-benzoxabismole (11). To a stirred solution of 2-C_6H_4(I)CMe_2-OMe (0.88 g, 3.19 mmol) in 10 mL of THF at −78 °C was added dropwise *n*-BuLi (3.56 mmol in 2.3 mL of hexane). The reaction mixture was stirred at the temperature for 30 min, and the solution was added to a cold solution of **6b** (1.56 g, 3.19 mmol) in 20 mL of THF. After the mixture was allowed to warm to room temperature, it was stirred for a further 10 h and then the reaction was quenched with water. Colorless crystals of **11** (0.55 g, yield 29%) were obtained after recrystallization from ether: mp 234-235 °C; ^{1}H NMR ($CDCl_3$) 1.56−1.63 (m, 6 H), 3.80 (s, 3 H), 7.10−7.90 (m, 7 H), 8.10−8.20 (m, 1 H); ^{19}F NMR ($CDCl_3$) −72.6 (q, J = 8.6 Hz, 3 F), −75.9 (q, J = 8.6 Hz, 3 F). Anal. Calcd for $C_{19}H_{17}F_6O_2Bi$: C, 38.01; H; 2.85. Found: C, 38.40; H; 2.82.

1-[2-(2-Methoxyhexafluoro-2-propyl)phenyl]-3,3-bis(trifluoromethyl)-3*H*-2,1-benzoxabismole (12). To a stirred solution of 2-C_6H_4(Br)$C(CF_3)_2$OMe (0.78 g, 3.19 mmol) in 5 mL of ether at −63 °C was added dropwise *n*-BuLi (2.32 mmol in 1.4 mL of hexane). The reaction mixture was stirred at the temperature for 2 h, and the solution was added to a cold solution of **6b** (0.99 g, 1.94 mmol) in 10 mL of ether. After the mixture was allowed to warm to room temperature, it was stirred for a further 10 h and then the reaction was quenched with water. The compound **12** was purified by column chromatography (*n*-hexane−CH_2Cl_2) to give colorless crystals (0.35 g, yield 26%): mp 220−222 °C dec; ^{1}H NMR ($CDCl_3$) 4.38 (s, 3 H), 7.25−7.96 (m, 7 H), 8.34 (d, J = 7.6 Hz, 1 H); ^{19}F NMR ($CDCl_3$) −67.1 (bq, 3 F), −67.6 (bq, 3 F), −72.5 (q, J = 8.6 Hz, 3 F), −76.2 (q, J = 8.6 Hz, 3 F). Anal. Calcd for $C_{19}H_{11}F_{12}O_2Bi$: C, 32.22; H, 1.56. Found: C, 32.44; H, 1.33.

1-[2-((*N*-Methylamino)methyl)phenyl]-3,3-bis(trifluoromethyl)-3*H*-2,1-benzoxabismole (13). To a stirred solution of *N*-methylbenzylamine (0.1 mL, 0.78 mmol) and TMEDA (0.05 mL, 0.38 mmol) in 9 mL of ether at −78 °C was added dropwise *n*-BuLi (1.66 mmol in 1.0 mL of hexane). The reaction mixture was stirred for 5 h, and the solution was added to a cold solution of **6b** (0.5 g, 1.02 mmol) in 10 mL of ether. After the mixture was allowed to warm to room temperature, it was stirred for a further 10 h and then the reaction was quenched with water. Pure **13** (0.10 g, yield 21%) was obtained after recrystallization from ether: mp 173−174 °C; ^{1}H NMR (acetone-d_6) 2.74 (d, J = 7.3 Hz, 3 H), 4.20 (dd, J = −14.8, 5.0 Hz, 1 H), 4.41 (dd, J = −14.8, 5.0 Hz, 1 H), 4.63 (brs, 1 H), 7.1−7.7 (m, 6 H), 7.9−8.1 (m, 2 H); ^{19}F NMR (acetone-d_6) −73.2 (q, J = 9.3 Hz, 3 F), −76.3 (q, J = 9.3 Hz, 3 F). Anal. Calcd for $C_{17}H_{14}F_6ONBi$: C, 35.74; H, 2.47; N, 2.45. Found: C, 36.04; H; 2.16, N, 2.51.

1-[2-(Methoxymethyl)phenyl]-3,3-bis(trifluoromethyl)-3*H*-2,1-benzoxabismole (14). To a stirred solution of *n*-BuLi (14.9 mmol in 9 mL of hexane) and TMEDA (0.1 mL, 1.21 mmol) was added a solution of benzyl alcohol (0.7 mL, 6.76 mmol) in 10 mL of ether at −78 °C dropwise. The mixture was allowed to warm to room temperature and was stirred for a further 15 h. A solution of **6b** (3.10 g, 6.1 mmol) in 20 mL of ether was added dropwise to a cold stirred solution of the lithium reagent at −78 °C, and the mixture was stirred for 6 h at −78 °C. After an excess amount of MeI (1 mL, 16 mmol) was added to the solution, the mixture was stirred for 15 h and then the reaction was quenched with water. Pure **14** (1.58 g, yield 60%) was obtained after recrystallization from CH_2Cl_2−MeOH: mp 195−196 °C, ^{1}H NMR ($CDCl_3$) 3.79 (s, 3 H), 4.71 (d, J = −12.8 Hz, 1 H), 5.11 (d, J = −12.8 Hz, 1 H), 7.13−7.80 (m, 7 H), 8.07 (d, J = 7.9 Hz, 1 H); ^{19}F NMR ($CDCl_3$) −76.9 (q, J = 8.4 Hz, 3 F), −80.0 (q, J = 8.4 Hz, 3 F). Anal. Calcd for $C_{17}H_{13}F_6O_2Bi$: C, 35.81; H, 1.93. Found: C, 35.68; H, 2.29.

1-[2-((*N*,*N*-Dimethylamino)methyl)phenyl]-3,3-bis(trifluoromethyl)-3*H*-2,1-benzoxastibole (15). To *N*,*N*-dimethylbenzylamine (0.15 mL, 0.99 mmol) in 5 mL of ether was added *n*-BuLi (0.98 mmol in 0.62 mL of hexane) dropwise at −78 °C. The solution was allowed to warm to room temperature, and stirring was continued overnight. After 2 mL of THF was added to dissolve the formed precipitate, the resulting solution was added dropwise via cannula at −78 °C to **7a** in 10 mL of ether prepared by treating **5a** (0.41 g, 1.00 mmol) with trifluoroacetic acid (0.2 mL, 2.6 mmol) in ether and removing the solvent and excess acid in vacuo. Stirring was continued for 1 h, after which the solution was allowed to warm to room temperature. After the reaction was quenched with water and the usual workup was performed, the residue was subjected to TLC (hexane−CH_2Cl_2 = 1:1). Recrystallization from hexane−CH_2Cl_2 afforded **15** as colorless needles (0.21 g, yield 42%): mp 164−166 °C; ^{1}H NMR ($CDCl_3$) 2.49 (bs, 3 H), 2.74 (bs, 3 H), 3.70 (d, J = 13.8 Hz, 1 H), 4.12 (d, J = 13.8 Hz, 1 H), 6.90−7.88 (m, 8 H); ^{19}F NMR ($CDCl_3$) −77.4 (q, J = 9.3 Hz, 3 F), −74.1 (q, J = 9.3 Hz, 3 F). Anal. Calcd for $C_{18}H_{16}F_6NOSb$: C, 43.41; H, 3.23; N, 2.81. Found: C, 43.50; H, 3.24; N, 2.58.

3-*tert*-Butyl-1,5-bis((dimethylamino)methyl)benzene. To a solution of 3-*tert*-butyl-1,5-bis(bromomethyl)benzene (3.70 g, 11.6 mmol) in 60 mL of THF were added 13.5 mL of triethylamine and dimethylammonium chloride (6.00 g, 73.6 mmol) at room temperature. The mixture was stirred for 12 h. The product was crystallized from EtOH−benzene (2.53 g, yield 88%): ^{1}H NMR ($CDCl_3$) 1.32 (s, 9 H), 2.23 (s, 12 H), 3.41 (s, 4 H), 7.04 (s, 1 H), 7.20 (s, 2 H).

1-{2,6-Bis[(dimethylamino)methyl]-4-*tert*-butylphenyl}-3,3-bis(trifluoromethyl)-3*H*-2,1-benzoxabismole (22). A solution of *n*-butyllithium (2.3 mmol) in hexane (1.4 mL) was added at room temperature to a solution of 3-*tert*-butyl-1,5-bis((dimethylamino)-methyl)benzene (550 mg, 2.21 mmol) and TMEDA (0.5 mL) in ether (20 mL). The resulting yellow solution was stirred for 20 h at room temperature and was added dropwise to a suspension of **6b** (711 mg, 1.4 mmol) in ether (20 mL) at −78 °C. The suspension was allowed to warm to room temperature and was stirred for a further 10 h. After addition of 20 mL of water and extraction with three 100 mL portions of ether, the combined organic layers were dried over anhydrous K_2CO_3. After filtration and evaporation of the filtrate, the residue was recrystallized from CH_2Cl_2−MeOH to give colorless crystals of **22** (420 mg, yield 43%): ^{1}H NMR (CD_2Cl_2, −70 °C) 1.11 (s, 9 H), 2.09 (s, 6 H), 2.56 (s, 6 H), 3.05 (d, J = −14.0 Hz, 2 H), 4.25 (d, J = −14.0 Hz, 2 H), 7.17 (s, 2 H), 7.29−7.33 (m, 1 H), 7.57−7.61 (m, 2 H), 7.93−7.95 (m, 1 H); ^{19}F NMR (CD_2Cl_2, −90 °C) −73.2 (brs, 6 F); ^{1}H NMR (CD_2Cl_2, 25 °C) 1.20 (s, 9 H), 2.38 (brs, 12 H), 3.09 (d, J = −13.0 Hz, 2 H), 4.43 (d, J = −13.0 Hz, 2 H), 7.23 (s, 2 H), 7.31−7.33 (m, 2 H), 8.00−8.03 (m, 2 H); ^{19}F NMR (CD_2Cl_2, 20 °C) −73.0 (s, 6 F). Anal. Calcd for $C_{25}H_{31}F_6ON_2Bi$: C, 42.99; H, 4.47; N, 4.01. Found: C, 42.80; H, 4.47; N, 4.20.

***m*-Bis((dimethylamino)methyl)benzene.** To 7 mL (159.0 mmol) of 90% formic acid in a 200 mL two-necked round-bottomed flask, cooled in ice water, was added slowly 5 mL of *m*-bis(diaminomethyl)-benzene (37.9 mmol). To the mixture were added 100 mL of water and a paraformaldehyde (4.55 g, 151.5 mmol) suspension. The flask was connected to a reflux condenser and was placed in an oil bath which had been heated to 90−100 °C. A vigorous evolution of carbon dioxide began after 2−3 min, at which time the flask was removed from the bath until the gas evolution notably subsided. Then it was placed again in the bath and heated under reflux for 8 h. After the solution had been cooled, aqueous potassium hydroxide was added, and the product was extracted with three 100 mL portions of benzene and dried over anhydrous granular potassium carbonate. The product was distilled at 70−72 °C (0.5 mmHg) to give a colorless liquid (6.52 g, yield 90%): ^{1}H NMR ($CDCl_3$) 2.23 (s, 12 H), 3.41 (s, 4 H), 7.18−7.27 (m, 4 H).

1-{2,6-Bis[(dimethylamino)methyl]phenyl}-3,3-bis(trifluoromethyl)-3*H*-2,1-benzoxabismole (23). A solution of *n*-butyllithium (6.6 mmol) in hexane (4 mL) was added at room temperature to a solution of 1,3-bis((dimethylamino)methyl)benzene (990 mg, 5.12 mmol) in ether (20 mL). The resulting yellow solution was stirred for 20 h at room temperature and then was added dropwise to a suspension of **6b** (2.61 g, 5.12 mmol) in ether (40 mL) at −78 °C. The suspension was allowed to warm to room temperature and was stirred for a further 3 h. After addition of 50 mL of water and extraction with three 100 mL portions of ether, the combined organic layers were dried over anhydrous K_2CO_3. After filtration and evaporation of the filtrate, the residue was recrystallized from CH_2Cl_2−MeOH to give colorless crystals of **23** (1.48 g, yield 45%): ^{1}H NMR (CD_2Cl_2, −55 °C) 2.10 (s, 6 H), 2.59 (s, 6

H), 3.09 (d, $J = -13.6$ Hz, 2 H), 4.34 (d, $J = -13.6$ Hz, 2 H), 7.14–7.22 (m, 3 H), 7.33 (dd, $J = 7.3$, 7.8 Hz, 1 H), 7.60–7.65 (m, 2 H), 7.99 (d, $J = 7.3$ Hz, 1 H); ^{19}F NMR (CD_2Cl_2, −90 °C) −75.84 (s, 6 F); ^{1}H NMR (CD_2Cl_2, 20 °C) 2.39 (brs, 12 H), 3.12 (d, $J = -13.6$ Hz, 2 H), 4.45 (d, $J = -13.6$ Hz, 2 H), 7.15–7.24 (m, 3 H), 7.33 (dd, $J = 7.3$, 7.3 Hz, 1 H), 7.62 (dd, $J = 7.3$, 7.3 Hz, 1 H), 7.69 (m, 1 H), 8.03 (d, $J = 7.3$ Hz, 1 H); ^{19}F NMR (CD_2Cl_2, 20 °C) −75.94 (s, 6 F). Anal. Calcd for $C_{21}H_{23}F_6ON_2Bi$: C, 39.26; H, 3.61; N, 4.36. Found: C, 39.26; H, 3.48; N, 4.41.

1-{2,6-Bis[(dimethylamino)methyl]phenyl}-3,3-bis(trifluoromethyl)-3*H*-2,1-benzoxastibole (24). To 1,3-bis((dimethylamino)methyl)-benzene (0.25 g, 1.32 mmol) in 10 mL of ether was added *n*-BuLi (1.32 mmol in 0.92 mL of hexane) at 0 °C. The solution was allowed to warm to room temperature and stirred additionally overnight. The resulting solution was added dropwise via cannula at −78 °C to **7a** prepared from 1-(4-methylphenyl)-3,3-bis(trifluoromethyl)-3*H*-2,1-benzoxastibole (0.40 g, 0.88 mmol) and trifluoroacetic acid (0.14 mL, 1.76 mmol). After being stirred at room temperature overnight, the solution was quenched with aqueous NH_4Cl. Workup was followed by short column chromatography (hexane−AcOEt = 1:1) of the residue. Recrystallization from MeOH−CH_2Cl_2 furnished **24** as colorless crystals (0.19 g, yield 38%): mp 164–165 °C; ^{1}H NMR (CD_2Cl_2, room temperature) 2.38 (bs, 12 H), 2.94 (d, $J = 14$ Hz, 2 H), 4.42 (d, $J = 14$ Hz, 2 H), 6.99 (d, $J = 7.3$ Hz, 2 H), 7.11 (t, $J = 7.3$ Hz, 1 H), 7.32 (t, $J = 7.3$ Hz, 1 H), 7.45 (t, $J = 7.3$ Hz, 1 H), 7.5–7.6 (m, 1 H), 7.91 (d, $J = 7.3$ Hz, 1 H); ^{19}F NMR (CD_2Cl_2, room temperature) −75.8 (bs, 6 F). Anal. Calcd for $C_{18}H_{16}F_6NOSb$: C, 45.43; H, 4.18; N, 5.05. Found: C, 45.53; H, 4.31; N, 4.82.

Crystallographic Studies. Crystal Structure of 10, 23, and 24. Crystal data and numerical details of the structure determinations are given in Table 9. Crystals suitable for X-ray structure determination were mounted on a Mac Science MXC3 diffractometer and were irradiated with graphite-monochromated Mo Kα radiation ($\lambda = 0.71073$ Å) for data collection. Lattice parameters were determined by least-squares fitting of 36 for **10**, of 31 for **23**, and of 39 reflections for **24** with $31° < 2\theta < 35°$, $26° < 2\theta < 30°$, and $31° < 2\theta < 44°$ for **10**, **23**, and **24**, respectively. Data were collected with the ω scan mode. All data were corrected for absorption[29] and extinction.[30] The structures were solved by a direct method with a program, Monte Carlo-Multan.[31] Refinement on F was carried out by full-matrix least-squares. All non-hydrogen atoms were refined with anisotropic thermal parameters. All hydrogen atoms in **24** could be found on a difference Fourier map; these coordinates were included in the refinement with isotropic thermal parameters. The hydrogen atoms in **10** and **23** were included in the refinement on calculated positions (C−H = 1.0 Å) riding on their carrier atoms with isotropic thermal parameters. All the computations were carried out on a Titan-750 computer.

Table 9. Crystal Data for **10**, **23**, and **24**

	10	**23**	**24**
formula	$C_{18}H_{16}F_6NOBi$	$C_{21}H_{23}F_6N_2OBi$	$C_{21}H_{23}F_6N_2OSb$
mol wt	585.30	642.5	555.3
cryst syst	monoclinic	triclinic	triclinic
space group	$P2_1/a$	$P\bar{1}$	$P\bar{1}$
cryst dimens, mm	0.50 × 0.50 × 0.20	0.25 × 0.20 × 0.12	0.40 × 0.30 × 0.10
a, Å	11.050(2)	9.341(4)	9.374(3)
b, Å	18.572(3)	10.273(4)	10.245(3)
c, Å	9.856(2)	12.693(3)	12.658(3)
α, deg	90	89.99(3)	89.89(2)
β, deg	108.21(1)	81.08(3)	82.31(2)
γ, deg	90	73.02(3)	71.48(2)
V, Å^3	1921.3(6)	1149.5(7)	1141.2(5)
Z	4	2	2
D_{calc}, g cm^{-3}	2.02	1.86	1.62
abs coeff, cm^{-1}	88.72	74.40	11.58
F(000)	1104	616	552
radiation; λ, Å	Mo Kα, 0.71073	Mo Kα, 0.71073	Mo Kα, 0.71073
temp, °C	23 ± 1	23 ± 1	23 ± 1
2θ max, deg	55	50	50
scan rate, deg/min	10.0	4.0	4.0
linear decay,%		4	
data collected	$\pm h,-k,\pm l$	$\pm h,\pm k,-l$	$\pm h,\pm k,+l$
total data collcd, unique, obsd	4921, 4407, 3588 ($I > 3\sigma(I)$)	4292, 4027, 3555 ($I > 3\sigma(I)$)	4286, 4022, 3753 ($I > 3\sigma(I)$)
R_{int}	0.06	0.03	0.03
no of params refined	250	286	355
R, R_w, S	0.060, 0.082, 1.15	0.050, 0.079, 1.97	0.026, 0.026, 1.76
max shift in final cycle	0.13	0.06	0.40
final diff map, max, e/Å^3	3.40	1.66	0.48

Acknowledgment. We are indebted for partial support of this research to Grant-in-Aids for Scientific Research on Priority Area of Organic Unusual Valency (Grants 02247103, 03233104, and 04217105) administered by the Ministry of Education, Science and Culture of the Japanese Government.

Supplementary Material Available: Tables of positional and thermal parameters and complete interatomic distances and angles for **10**, **23**, and **24** (41 pages). This material is contained in many libraries on microfiche, immediately follows this article in the microfilm version of the journal, can be ordered from the ACS, and can be downloaded from the Internet; see any current masthead page for ordering information and Internet access instructions.

JA944038L

(29) Furusaki, A. *Acta Crystallogr.* **1979**, *A35*, 220.
(30) Katayama, C. *Acta Crystallogr.* **1986**, *A42*, 19.
(31) Coppens, P.; Hamilton, W. C. *Acta Crystallogr.* **1970**, *A26*, 71.
(32) The Bi−O dissociative mechanism for the CF_3 exchange is considered to be impossible because both CF_3 groups should still be diastereotopic even after Bi−O dissociation because bismuth atom is asymmetric (only inversion at the central bismuth atom can cause the exchange of the CF_3 groups). Since we did not observe the diastereotopicity of the CF_3 groups in several solvents at any higher temperatures (for example, −70 to 100 °C in **24**) even by 400 MHz NMR, the phenomenon we observed must be caused by inversion at the central bismuth (or antimony) atom.